Tunable Differential Interferometer For Optical Tomography

Faris, G. W; Hertz, H. M

Published in:
Optical Society of America. Journal B: Optical Physics

DOI:
10.1364/AO.28.004662

1989

Tunable differential interferometer for optical tomography

Gregory W. Faris and Hans M. Hertz

We report the use of a tunable differential interferometer for optical tomography. This interferometer has several advantages over other methods for phase measurements in optical tomography, including good stability, variable sensitivity, and the elimination of fringe ambiguity. Quantitative images of the gas concentrations in subsonic jets of methane and oxygen issuing into air are presented, with absolute accuracies better than 3.5% and 4.5%, respectively.

I. Introduction

The tomographic technique has become well established as a method for quantitative optical imaging using integrated measurements of phase,[1,2,3] absorption,[4,5] or emission.[6] While integrating measurements readily yield accurate quantitative measurements, spatial information is lost in the direction of integration. The lost information can be retrieved by taking multiple sets of integrated measurements (called projections) at different angles through an object or field of interest and using a tomographic algorithm[7] to reconstruct a section through the object.

Optical tomography using phase measurements has the advantage of operating far from an optical resonance, thus being applicable to any transparent system and not requiring a tunable laser. Phase measurement techniques applied to optical tomography include conventional interferometric,[1] beam deflection,[2] and holographic[3] techniques. Holograhic data recording has the disadvantage that the holograms must be digitized prior to reconstruction on a computer. Interferometric[1] and beam deflection[2] measurements have been performed with elecronic data recording, allowing direct transfer of the data to a computer. However, present implementations of these techniques suffer from drift and slow data acquisition, respectively. In this paper we present a tunable stable differential interferometer which combines the advantages of the beam deflection method with efficient parallel data recording.

A differential interferometer[8] (also called a shearing or polarization interferometer) is different from most other interferometers in that both of the interfering optical waves pass through the object being examined. The waves are distinguished by their differing polarizations. A transverse displacement between the two polarizations is created by a birefringent element and the resulting interference pattern depends on the gradient in the path-integrated phase through the object.

A differential interferometer has several advantages for use in optical tomography. Because the interfering waves travel over nearly the same paths, a differential interferometer is more stable than interferometers that have physically separate signal and reference waves. Additionally, by varying the separation between the two polarizations, the sensitivity may be varied to match the size of the signal, thus maximizing the useful dynamic range. Furthermore, because a differential interferometer measures the gradient of the optical path length, it has some of the advantages of beam deflection measurements for tomography,[9] including favorable scaling properties (i.e., the signal scales with the peak index of refraction, not with the size of the object), a good spatial frequency content for reconstruction (leading to high frequency noise reduction), and the possibility of eliminating fringe ambiguity.

Tomographic measurements were performed previously using a differential interferometer.[10] However, the Wollaston prism interferometer used for those measurements could only be tuned by exchanging prisms. The sensitivity of the continuously tunable interferometer described here may be easily varied to optimize the signal-to-noise ratio for the object under study. For the different objects measured here, we adjusted the interferometer to yield signal variations which are close to, but less than, a fringe. For such single fringe measurements there is no uncertainty in

When this work was done both authors were with Lund Institute of Technology, Physics Department, S-221 00 Lund, Sweden. Gregory Faris is now with SRI International, Molecular Physics Laboratory, 333 Ravenswood Avenue, Menlo Park, California 94025, and Hans Hertz is now with Stanford University, Ginzton Laboratory of Physics, Stanford, California 94305.

Received 15 March 1989.
0003/6935/89/214662-06$02.00/0.

the sign of the phase change across a fringe. This is important for the study of random flows where clues to the direction of phase variation across an interference fringe may be absent. Additionally, because there is no fringe ambiguity, a computer can make unassisted fringe assignments of arbitrary test objects. Complete computer control of the data processing is important for optical tomography, especially when a large amount of data is involved, such as would be the case for high frame rate measurements of time-dependent flows, for example. For tomographic measurements with the differential interferometer described here, the projections were recorded with a diode array and could be transferred directly into a computer for data processing and reconstruction. The differential interferometer has been operated with sensitivity to gradients in the plane to be reconstructed, allowing direct reconstruction of the index of refraction.[9] The index of refraction may then be related to temperature,[1,11] density[2] or concentration.[3,11]

II. Tunable Differential Interferometer

A diagram of the interferometer used for the measurements described here is shown in Fig. 1. The birefringent element used for separation of the two polarizations is a calcite crystal. The crystal is 20 mm long in the direction of light propagation, antireflection coated, and polished to $\lambda/5$ wavefront distortion. The optic axis is oriented vertically and the crystal is tilted by an angle θ in the horizontal plane. When light polarized at 45° to the vertical passes through the crystal, the horizontally and vertically polarized components are displayed by different distances. Thus, the crystal superimposes beams of perpendicular polarizations which have traveled parallel paths through an object being examined, separated by a distance Δx. The orthogonally polarized waves are resolved for a common polarization direction at 45° to the vertical with an antireflection coated cube beam splitter. When the two displaced waves interfere on the detector, the result is a function of the gradient in the path-integrated index of refraction. The sensitivity of the interferometer depends on the separation between the two polarizations Δx, which may be easily varied by changing the tilt angle θ of the crystal.

The light source used for the interferometer is a polarized He–Ne laser and a halfwave plate to control the orientation of the polarization. A sheet of laser light is formed with a 6-mm focal length cylindrical lens and a 1-m focal length mirror. To minimize the effects of shadowgraph patterns on the intensity distribution at the detector, the center of the flow field is imaged onto the detector with a second 1-m focal length mirror, the image being magnified by a factor of 1.2. The detector used is an EG&G OMA intensified photodiode array. An intensified diode array is not necessary for these measurements but the OMA system was the only suitable diode array available. Neutral density filters with an optical density of 6 are placed in front of the detector to reduce the intensity, giving a factor of 1000 times more attenuation than the

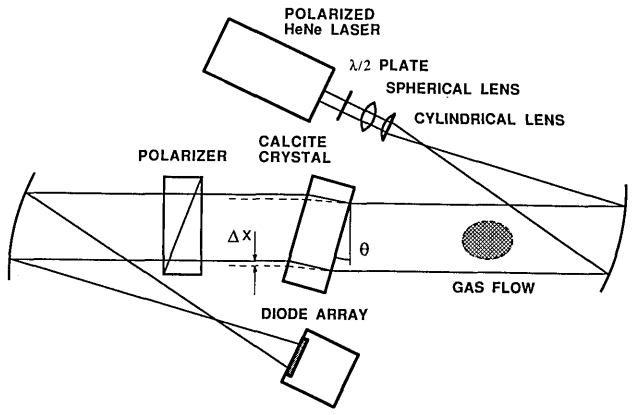

Fig. 1. Experimental arrangement for the tunable differential interferometer.

gain of the image intensifier. Because the diode elements are 2.5 mm high, they do not define a narrow vertical resolution in the object plane. To this end, a 1-m focal length spherical lens is used to reduce the height of the light sheet in the flow field under study to a full width at half-maximum of 400 μm. Use of a photodiode array with shorter elements would easily reduce the vertical resolution to below 100 μm without using such a lens.

The horizontal resolution is limited by the separation between the two orthogonally polarized waves. For the measurements of methane and oxygen flows described below, this separation is 102 and 220 μm, respectively. Geometric effects[9] and a running average of the data to reduce the number of points prior to tomographic reconstruction limited the horizontal resolution in the projections to 170 and 220 μm, respectively. Because the flows studied are slowly varying with respect to aximuthal rotation, this is representative of the horizontal resolution in the reconstructions.

The intensity distribution at the detector, $I(x)$, may be expressed as

$$I(x) = I_0(x) \sin^2 \{\tfrac{1}{2}[\phi_\theta + \phi_{\mathrm{err}}(x) + \phi_{\mathrm{sig}}(x)]\}, \quad (1)$$

where $I_0(x)$ is the incident intensity, and ϕ_θ, $\phi_{\mathrm{err}}(x)$, and $\phi_{\mathrm{sig}}(x)$ are the phase difference between the interfering beams due to the crystal tilt angle θ, the phase error or nonuniformity due to the crystal's wavefront distortion, and the differential phase signal from the object, respectively. The procedure for evaluation of the object-dependent phase ϕ_{sig} from the measured intensity $I(x)$ is illustrated in Fig. 2. A typical measurement of a phase object (actually one of the projections for the image presented in Fig. 3 below) is shown as I_{sig} in Fig. 2(a). A background distribution measured with the laser blocked has been subtracted from this curve and the other curves shown in Fig. 2(a). Two additional intensity distributions are required for calibration of the interferometer. One, marked I_{ref} in Fig. 2(a), is taken with the same conditions as I_{sig}, except without a phase object present. Another measurement with no phase object is taken with the input polarization rotated 90° using the halfwave plate. The sum of this curve and the I_{ref} curve yields the

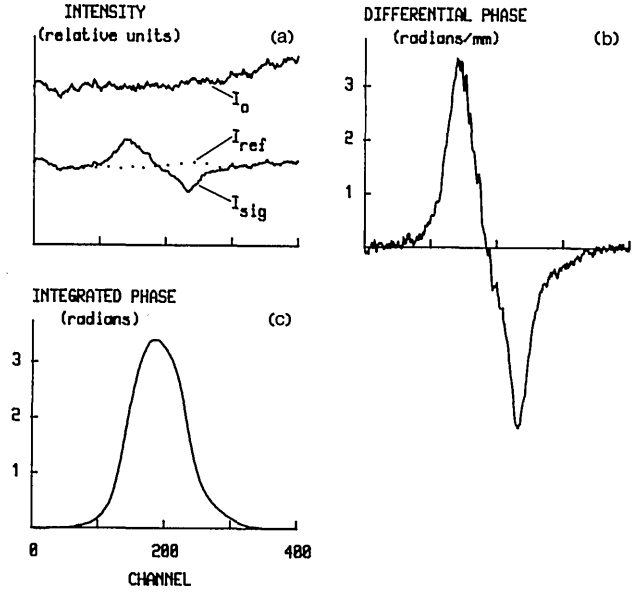

Fig. 2. Typical projection measurements for the differential interferometer: (a) signal (I_{sig}), reference (I_{ref}), and incident intensity (I_0) curves; (b) differential projection, calculated from the curves in (a); (c) projection, resulting from the integration of the curve in (b).

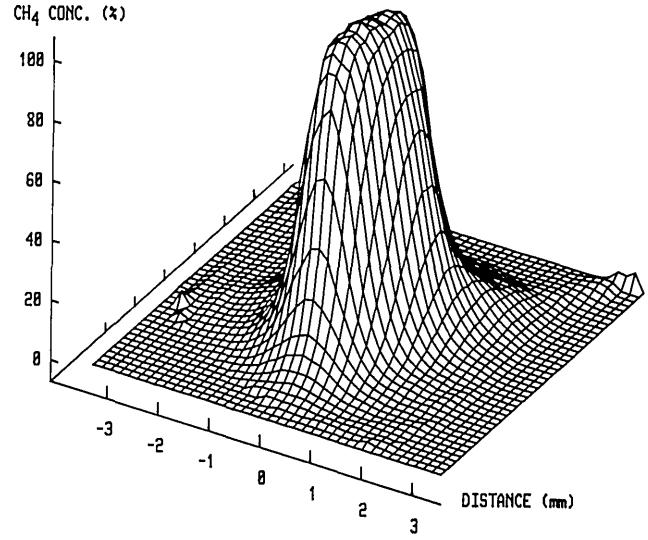

Fig. 3. Tomographic reconstruction of the concentration of methane in a subsonic asymmetric jet into air; the pixel size is 160 × 160 μm.

incident intensity distribution, marked as I_0 in Fig. 2(a). This technique using a halfwave plate for measuring $I_0(x)$ involves minimal perturbation of the intensity distribution from the distribution that is actually present during a measurement.

Using Eq. (1), it is easily shown that the differential phase for the object is

$$\phi_{sig}(x) = 2\sin^{-1}\left[\frac{I_{sig}(x)}{I_0(x)}\right]^{1/2} - 2\sin^{-1}\left[\frac{I_{ref}(x)}{I_0(x)}\right]^{1/2}. \quad (2)$$

Note that the phase errors due to crystal wavefront distortion $\phi_{err}(x)$ are automatically eliminated in the measurement procedure. The phase distribution calculated from the curves in Fig. 2(a) is shown in Fig. 2(b). Integration of this curve yields the total phase shift given in Fig. 2(c).

Calibration of the differential interferometer is required to obtain quantitative measurements. This involves measurement of the separation between the polarizations Δx and the magnification of the image. These can be measured accurately optically using the diode array and a razor blade positioned in the object plane. The magnification is measured by moving the razor blade with a micrometer-driven translation stage and measuring the number of pixels the razor blade image moves on the array. Similarly, the separation between the polarizations is calculated from the number of pixels the razor image moves when using the halfwave plate to alternate between horizontally and vertically polarized light. This measurement agrees well with the separation calculated using the crystal thickness, the refractive indices for calcite and the tilt angle θ. The latter is a more accurate technique for measurement of small polarization separations. The ability to vary the input polarization is also helpful for aligning the optic axes of the crystal and polarizer to obtain good extinction. This was done through iterative adjustment of the halfwave plate, the crystal, and the cube beam splitter for best extinction, with the polarization at 45° to alternate sides of vertical.

III. Experiment

We used this differential interferometer to examine laminar flows of methane and oxygen issuing vertically from a nozzle into the ambient atmosphere. A rectangular nozzle and circular nozzle were used, each constructed to give a laminar flow with a nearly uniform velocity distribution. The rectangular nozzle has a 1.25- × 2.5-mm orifice. The orifice of the circular nozzle is 4 mm in diameter. Because the flows are steady state, the measurements could be performed with a single interferometer by rotating the nozzle between each projection. For each projection, fifty scans of the diode array were averaged, with a 16.6-ms exposure time for each scan.

We took a small number of projections (six) for each of the reconstructions described here. For tomographic reconstructions from a small number of projections, an iterative reconstruction technique yields smaller artifact errors than an analytic technique, such as the convolution backprojection algorithm. We used an iterative technique for tomographic reconstruction, a modified version of the MART algorithm, which is described in Ref. 12. When the calibrations described in Sec. II are used, the reconstructions yield 2-D images of the index of refraction. Using refractive index data from Ref. 13 for the flowing gases (methane and oxygen) and from Ref. 14 for air, the refractive index values were related to spatially resolved gas concentrations. The refractive indices were calculated for the He–Ne wavelength and further corrected for ambient temperature, pressure, and humidity.

Figure 3 shows a tomographic reconstruction of the methane concentration in a jet of that gas flowing at 1.3

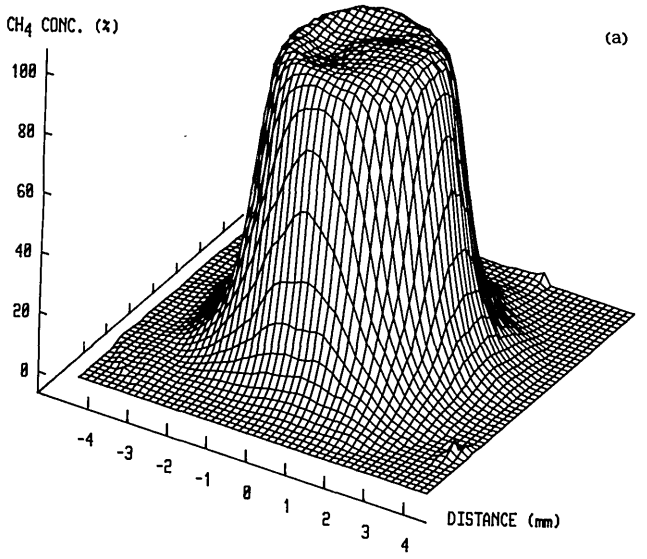

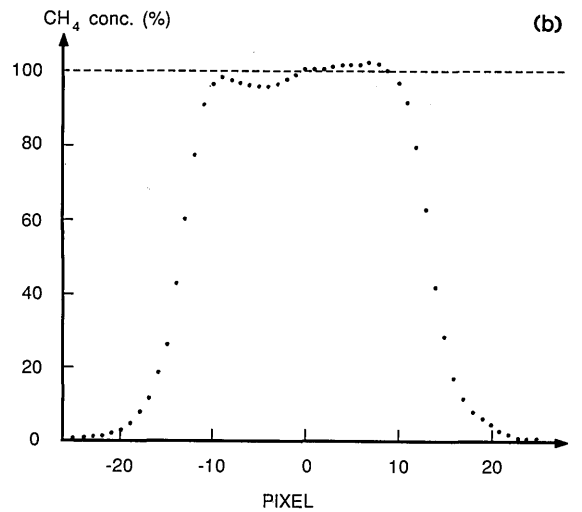

Fig. 4. (a) Tomographic reconstruction of a cylindrical methane jet; the pixel size is 160 × 160 μm. (b) Section through the center of the reconstruction in (a).

liter/min from the rectangular nozzle. The measurements were performed 3 mm above the nozzle orifice. The separation Δx between the interfering beams was 102 μm and the pixel spacing in the image is 160 × 160 μm. The average methane concentration in the flat, central region is 101%.

The cylindrical nozzle was used to check the accuracy of the reconstruction from the differential interferometer. By performing measurements 0.5 mm above the orifice the effects of diffusion and entrainment of air on the concentration present in the central flow were minimized. A reconstruction of a 1.8 liter/min flow of methane from the nozzle is shown in Fig. 4(a). A section through the center of the reconstruction is shown in Fig. 4(b). The average methane concentration in the flat region is 99.2% with a standard deviation of 1.8%. The estimated absolute accuracy of the concentrations in this image is better than 3.5% of the peak concentration. Sources of error are discussed in Sec. IV.

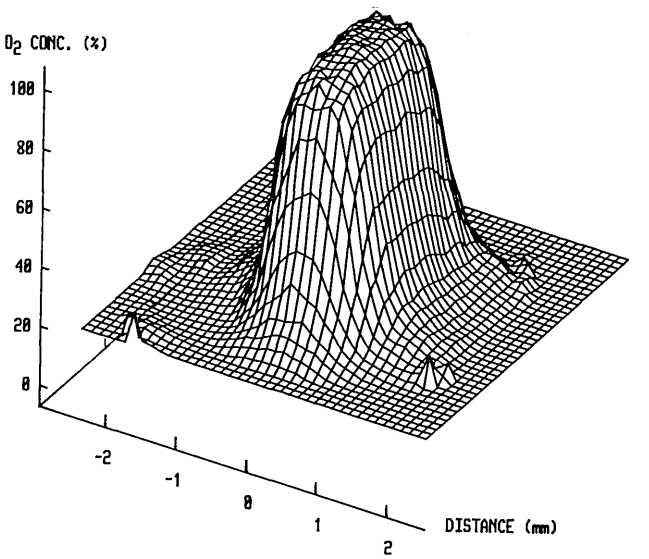

Fig. 5. Tomographic reconstruction of the oxygen concentration in an asymmetric jet into air; the pixel size is 115 × 115 μm.

To demonstrate the versatility of the interferometer, a flow of oxygen from the rectangular nozzle was examined. The difference in refractive index between oxygen and air is 7 times less than the refractive index difference for methane and air. The separation between the two polarizations was increased to 220 μm to obtain a sufficient signal to noise ratio. Measurements were performed at a height of 0.5 mm above the nozzle with a flow of 0.95 liter/min. Although the largest signal in the integrated projections from these measurements corresponds to only 0.08 of an optical wave, the quality of the reconstruction is good. The reconstructed oxygen concentration is shown in Fig. 5. The average oxygen concentration in the flat region of the reconstruction is 103%.

IV. Discussion

The differential interferometer we used is unusual in that there is a large difference in optical path length through the crystal for the two orthogonally polarized waves. The advantage of the interferometer is the simple design and the ease of tuning the sensitivity. Using a laser as the light source yields a coherence length more than adequate for measurements with the optical path length difference, which for our interferometer was equivalent to 3.4 mm in air.

Because of the optical path length difference, the image planes for the two polarizations are separated in the direction of light propagation. This separation causes an error in the differential projection whose magnitude depends on the size of the angle a given light ray is deflected by the gradients of the flow. For the flows investigated here, with deflection angles up to 0.54 mrad, the largest errors in the differential projections are 0.9%. The errors in the integrated projections are 50–80% of this value. Spherical aberration through the titled crystal is another source of error.

Spherical aberration errors were calculated to be 0.08% and 1.7% for the methane and oxygen reconstructions, respectively. In principle, the errors due to both offset image planes and spherical aberration can be corrected computationally.

In the above measurements, the vertical gradients are small compared with the horizontal gradients. However, in general, a phase object may have both horizontal and vertical gradients. The vertical gradients will, to a small extent, also contribute to the signal since the resulting change in the vertical angle of incidence on the crystal changes the phase difference between the two polarizations through the crystal. For a horizontal polarization separation Δx of 100 μm, the signal due to vertical gradients corresponding to a 1-mrad vertical deflection was calculated to be <1% of the signal from an equally large horizontal gradient. Using a thinner crystal and a larger tilt angle to achieve the same polarization separation would reduce the errors due to the offset image planes (discussed in the preceding paragraph) and the potential errors for vertical deflections but increase the spherical aberration. However, larger crystal angles also tend to increase the errors due to crystal wavefront distortion (ϕ_{err}), thus increasing the variation in the reference phase [e.g., curve I_{ref} in Fig. 2(a)]. As the variation in the reference phase increases, the measurement range available to perform single fringe measurements is reduced.

The total errors in the reconstructions of methane and oxygen jets have been estimated to be better than 3.5% and 4.5% of the peak values, respectively. Reconstruction errors contribute an error of ~2%.

In using this interferometer with signals of less than a fringe, care has to be taken to avoid unwanted fringes from reflections and scattering, as they are sources of error. For this experiment, the calcite crystal, the halfwave plate, and the cube beam splitter were antireflection coated. Additionally, index matching fluid was placed between the neutral density filters in front of the diode array and the 1-m lens was tilted slightly. An alternative method to prevent errors from fringes is to use a light source with a much shorter coherence length. In this case it would be necessary to use a second, compensating birefringent crystal before the flow field or phase object to balance the optical lengths for the two polarizations.

The differential interferometer proved to be very insensitive to mechanical vibration. However, temperature variations lead to expansion or contraction of the crystal, thus varying the phase offset $\phi_\theta + \phi_{\text{err}}$ in Eq. (1). Stabilization against temperature changes is much simpler than for a conventional interferometer because the interferometer is only sensitive to temperature changes in the crystal itself. For the single fringe measurements described above, isolation of the crystal from room air currents resulted in sufficient stability for good measurements.

For single fringe measurements, this interferometer produces images similar to those of a schlieren system. The optical setup is quite similar to that for schlieren and would be a good alternative technique when quantitative rather than qualitative measurements are desired.

An interesting variation of the interferometer would allow measurement of I_0 simultaneously with the measurement of a phase object. This could be done by imaging either the orthogonal polarization (that rejected by the cube beam splitter) or both polarizations (by placing a beam splitter between the object and the crystal) onto a second diode array. This would be useful when the incident intensity I_0 were not sufficiently stable, as might be the case for pulsed sources or for a stable I_0, this would allow measurement of both absorption and phase. Knowledge of both the integrated phase and absorption could allow reconstruction for two parameters, such as both temperature and concentration for simple systems, or allow for better correction of phase or absorption effects in a single parameter reconstruction.

Various properties of the projections produced with this differential interferometer make them well suited to analog tomographic reconstruction.[15] Analog reconstruction techniques have the potential of being extremely fast and do not require a computer. Analog reconstruction techniques typically involve an optically performed filtering process and an integration onto a detector or film. The projections from the differential interferometer are well suited for Fourier optical processing for several reasons: the required filter for these transverse gradient projections is very simple[9]; the entire projection is measured simultaneously; and the projection values are present in the form of a coherent optical signal whose values are linearly proportional to the line integrals in the projection (when the sensitivity is adjusted to make the signals small compared to the full dynamic range).

Differential interferometers with transverse polarization separation yield transverse gradient projections such as those for beam deflection measurements. Reconstruction of transverse gradient projections results in high frequency noise reduction relative to ordinary projections. This is discussed in detail in Ref. 9 along with a form of the convolution backprojection reconstruction algorithm for direct reconstruction from this type of projection. Although the MART algorithm used here performs on ordinary projections, reduction of high frequency noise occurs in the integration of the measured projection [i.e., Fig. 2(b)] to give a projection suitable for the MART algorithm [i.e., Fig. 2(c)]. It would be of interest to examine the performance of an iterative algorithm designed to reconstruct transverse gradient projections directly.

V. Conclusions

The tunable differential interferometer presented here has many good qualities for optical tomography measurements. The variable sensitivity is an advantage over conventional or holographic techniques for tomography. Advantages due to the transverse gradient projections produced are high frequency noise reduction and the ability to scale to large systems. The single optical system described here may be extended

to allow more sophisticated measurements. A system of many such interferometers could perform instantaneous tomographic measurements. The stability, efficient electronic data processing, freedom of fringe ambiguity, and simultaneous acquistion of an entire projection make this differential interferometer well suited for such measurements. Use of a pulsed diode laser as a light source could reduce the temporal resolution to of the order of a microsecond. Exchange of the 1-D photodiode array for 2-D arrays would allow simultaneous acquisition of 3-D images.

The support of Sune Svanberg is gratefully acknowledged. This project was partially financed by the National Science Foundation, the Carl Trygger Foundation, and the Swedish Board for Technical Development.

References

1. H. M. Hertz, "Experimental Determination of 2-D Flame Temperature Fields by Interferometric Tomography," Opt. Commun. **54,** 131–136 (1985).
2. G. W. Faris and R. L. Byer, "Quantitative Three-Dimensional Optical Tomographic Imaging of Supersonic Flows," Science **238,** 1700–1702 (1987).
3. R. Snyder and L. Hesselink, "Measurement of Mixing Fluid Flows with Optical Tomography," Opt. Lett. **13,** 87–89 (1988).
4. G. W. Faris and R. L. Byer, "Quantitative Optical Tomographic Imaging of a Supersonic Jet," Opt. Lett. **11,** 413–415 (1986).
5. S. R. Ray and H. G. Semerjian, "High-Speed Laser Tomographic Measurements in Fluctuating Flames," in *Technical Digest, Conference on Lasers and Electro-Optics* (Optical Society of America, Washington, DC, 1985), paper TUB4.
6. H. M. Hertz and G. W. Faris "Emission Tomography of Flame Radicals," Opt. Lett. **13,** 351–353 (1988).
7. S. R. Deans, *The Radon Transform and Some of Its Applications* (Wiley, New York, 1983).
8. M. Francon, *Optical Interferometry* (Academic, New York, 1966) Chap. 7.
9. G. W. Faris and R. L. Byer, "Three-Dimensional Beam Deflection Optical Tomography of a Supersonic Jet," Appl. Opt. **27,** 5202–5212 (1988).
10. K. R. Kirchartz, U. Muller, H. Oertel, Jr., and J. Zierep, "Axisymmetric and Non-Axisymmetric Convection in a Cylindrical Container," Acta Mech. **40,** 181–194 (1981).
11. G. W. Faris and R. L. Byer, "Beam-Deflection Optical Tomography of a Flame," Opt. Lett. **12,** 155–157 (1987).
12. H. M. Hertz, "Kerr Effect Tomography for Nonintrusive Spatially Resolved Measurements of Asymmetric Electric Field Distributions," Appl. Opt. **25,** 914–921 (1986).
13. J. Bartels *et al.*, Eds., *Landolt-Bornstein: Zahlenwerte und Funktionnen, Vol. 2* (Springer-Verlag, Heidelberg, 1962).
14. B. Edlén, "The Refractive Index of Air," Metrologia **2,** 71–80 (1966).
15. H. H. Barrett and W. Swindell, "Analog Reconstruction Methods for Transaxial Tomography," Proc. IEEE **65,** 89–107 (1977).

FOURTH INTERNATIONAL SYMPOSIUM ON NONDESTRUCTIVE CHARACTERIZATION OF MATERIALS: June 11-14, 1990, Annapolis, MD. Contact: Robert E. Green, Jr. Johns Hopkins University, Center for NDE, Maryland Hall, Room 102, Baltimore, MD 21218. 301-338-7126.

In nature of background, this symposium is the fourth in the series that began in 1983 in Hershey, PA, became an international meeting in 1986 with the Montreal meeting and then met in 1988 in Saarbrucken, Germany.

The objective of these symposia is to provide a specific unique focus on the science and technology of nondestructive measurements applied to materials characterization. This includes microstructure, residual stress, dislocation density and distribution, etc. These symposia have functioned to gather together the technologists of nondestructive techniques with the mechanical and materials engineers to help explore solutions and applications of nondestructive characterization (NDC).

Contributed papers are welcome. Deadline: January 31, 1990. Submit to C.O. Ruud, 159 Materials Research Laboratory, The Pennsylvania State University, University Park, PA 16802.